# Potentials of mean force fail to describe chemical bond-breaking in solution

Cite as: J. Chem. Phys. 163, 154505 (2025); doi: 10.1063/5.0287220 Submitted: 23 June 2025 · Accepted: 12 September 2025 ·







**Published Online: 17 October 2025** 

Hannah Y. Liu, D Kenneth J. Mei, D William R. Borrelli, D and Benjamin J. Schwartz



# **AFFILIATIONS**

Department of Chemistry & Biochemistry, University of California, Los Angeles, Los Angeles, California 90095-1569, USA

Note: This Paper is Part of the Special Topic, Simulation of Excited State Dynamics in Molecular and Condensed-Matter Systems. a) Author to whom correspondence should be addressed: bjs@g.ucla.edu

#### **ABSTRACT**

Many liquid phase studies assume that the potential energy surfaces of reacting molecules are the same as in the gas phase, neglecting complex solvent dynamics that can completely alter the nature of chemical reactivity. Even studies that include solvent effects typically only consider them in an average, equilibrium way as part of a potential of mean force (PMF). In this work, we use mixed quantum/classical simulations to compare how equilibrium and non-equilibrium solvent motions affect the photodissociation of a simple diatomic molecule, NaK<sup>+</sup>, in liquid tetrahydrofuran. A PMF analysis shows that as the excited-state molecule dissociates with the solvent at equilibrium, the bonding electron remains associated with K<sup>+</sup> at short bond distances but eventually localizes on Na<sup>+</sup> at the end of dissociation. When we examine non-equilibrium dynamical photodissociation trajectories, however, we find that they fall into three distinct categories: about a quarter of them have the bonding electron mainly associated with  $Na^+$ , another quarter stay mainly associated with  $K^+$ , and about half have the bonding electron shared roughly equally between the two ions. The results show that equilibrium PMFs cannot accurately describe the dynamics of bond-breaking chemical reactions in solution because there is insufficient time for the solvent to reach equilibrium on the time scale over which bond dissociation occurs. Our analysis shows that the solvent coupling between the electronic energy surfaces is similar at and away from equilibrium, suggesting that other factors, such as solute velocity-driven solvent memory effects, play a more important role in explaining the failure of the equilibrium PMF to predict the non-equilibrium dynamics.

Published under an exclusive license by AIP Publishing. https://doi.org/10.1063/5.0287220

### I. INTRODUCTION

Quantum mechanical calculations have been able to do an outstanding job of providing a fundamental understanding of chemical reactions in the gas phase. 1-3 Since the reactants are isolated in a vacuum, potential energy surfaces (PESs) can be used to describe equilibrium molecular structures, transition states, reaction pathways, etc.4 However, most chemical reactions take place in solutionphase environments, and solvent effects can significantly alter the chemical properties of molecules compared to their gas-phase counterparts. In particular, the inevitable collisions between a reacting solute and the surrounding solvent molecules can have a dramatic effect on bond-breaking and forming processes in solution.

In previous work, we found that even weakly interacting solvents, such as liquid Ar, are capable of altering the vibrational frequencies of simple diatomics, such as Na<sub>2</sub> or Na<sub>2</sub><sup>+</sup>. <sup>11-13</sup> This is due to the fact that the surrounding Ar atoms confine these molecules' bonding electrons within a solvent cavity, increasing the

internuclear bonding electron density, decreasing the bond length, and increasing the vibrational frequency. 10-12 In addition, changing the solvent can produce different effects. 14,15 Solvents such as tetrahydrofuran (THF) can form dative bonds with the alkali metal cation cores inside these molecular solutes, creating discrete coordination structures that have different spectroscopic signatures and interconversion barriers of several  $k_BT$  so that they must be treated as separate molecular species. 11,12 Placing a gas phase system into solution can also shift the location of non-adiabatic curve crossings, 16-18 induce coupling between electronic states, 19 change the number and magnitude of energy barriers during reactions,<sup>20</sup> alter steric effects present in the gas phase,<sup>21</sup> and transform reaction coordinates.23

For heteronuclear diatomics, such as the NaK<sup>+</sup> molecule studied in this work, we found previously that solvation in liquid THF changes the thermodynamic products of dissociation.<sup>23</sup> Figure 1 compares the ground state (solid curves) and first electronic excited state (dashed curves) PESs of the NaK+ molecule in the gas phase

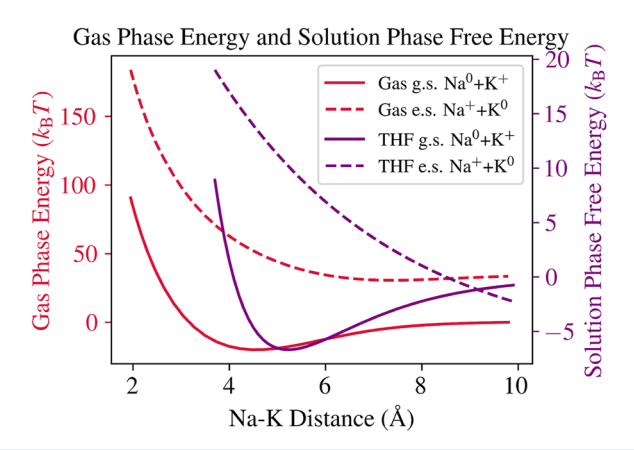


**FIG. 1.** Potential energy surfaces of the NaK<sup>+</sup> molecule in the gas phase (red curves, left *y*-axis) and potentials of mean force (PMFs) in room-temperature THF solution (purple curves, right *y*-axis).<sup>23</sup> Solid curves indicate the electronic ground state, and dashed curves indicate the lowest electronic excited state. In the asymptotic region in the gas phase, the ground-state (Na<sup>0</sup> + K<sup>+</sup>) and excited-state (Na<sup>+</sup> + K<sup>0</sup>) products are ~860 meV (~33.7  $k_{\rm B}T$  at room temperature) apart in energy,<sup>27.28</sup> which is the difference in the ionization energies of Na and K. In the solution-phase PMFs,<sup>23</sup> the gas-phase ground-state products are set to the zero of energy (solid purple curve). The PMFs for the ground and first excited states cross around 9 Å due to more thermodynamically favorable Na<sup>+</sup>–THF interactions in the dissociation limit.<sup>23</sup>

(red curves, left axis) and the potentials of mean force (PMFs) in liquid THF (purple curves, right axis). The NaK<sup>+</sup> molecule in the gas phase dissociates as Na<sup>0</sup> + K<sup>+</sup> and Na<sup>+</sup> + K<sup>0</sup> on its ground and first excited electronic states, respectively.  $^{24-26}$  This is due to the ~860 meV greater electron affinity of Na<sup>+</sup> relative to K<sup>+</sup>.  $^{27,28}$  Dissociation of NaK<sup>+</sup> in THF, on the other hand, reverses which products are formed. On the ground state, Na<sup>+</sup> + K<sup>0</sup> is now thermodynamically more stable due to more favorable Na<sup>+</sup>–THF interactions.  $^{23}$  In addition, the solvent-induced inversion of the thermodynamic dissociation products induces a crossing of the ground- and excited-state free energy surfaces at a bond distance of ~9 Å, suggesting that a long-range charge transfer process could occur during excited-state dissociation of this molecule.  $^{23,29,30}$ 

Solution-phase PMFs are calculated by assuming that the solvent molecules are fully equilibrated at every bond distance along the dissociation coordinate.<sup>31</sup> In other words, the PMFs in Fig. 1 are constructed assuming that the local THF solvent molecules have infinite time to respond to the elongation of the Na–K bond. However, during a bond-breaking reaction, the timescale of solvent relaxation could be comparable to or even longer than that of bond dissociation. If there is inadequate time for the solvent to respond and equilibrate during the reaction process, then the equilibrium-based PMFs may fail to describe bond-breaking reaction dynamics in solution.

In this work, we use mixed quantum/classical (MQC) molecular dynamics (MD) simulations to study the bond-breaking of the NaK<sup>+</sup> molecule in liquid THF both with the solvent at equilibrium and following non-equilibrium photodissociation. We find that the non-equilibrium and equilibrium solvent motions associated with dissociation are different enough that only about a quarter of the non-equilibrium trajectories follow the equilibrium predictions as

to which products are formed; in other words, non-equilibrium photodissociation produces different reaction products than those predicted by the equilibrium PMF ~75% of the time. This is because the time scale for solvent molecules to reach equilibrium is longer than the dissociation time of solution-phase NaK $^+$ . As a result, the solvent configurations in some photodissociation trajectories cause the bonding electron to associate with Na $^+$  without time for the THF solvent molecules to equilibrate and favor charge localization on K $^+$ . We also find that whether the non-equilibrium trajectories follow the reaction outcome predicted at equilibrium is correlated with the extent to which the Na and K first-shell solvent coordination numbers follow equilibrium predictions. Overall, we find that non-equilibrium solvation dynamics have a direct impact on the choice of chemical products for simple photodissociation reactions in solution.

#### II. METHODS

The details of our simulations are described in the supplementary material and are similar to the procedures used in Refs. 10, 12, 23, and 32. Briefly, we use MQC MD simulations to propagate non-equilibrium excited-state photodissociation trajectories. Our simulation box is cubic with a side length of 32.5 Å and contains 254 classical THF solvent molecules<sup>33</sup> and one NaK<sup>+</sup> solute. The solute's nuclear components (Na<sup>+</sup> and K<sup>+</sup> cations) are treated classically using pair-wise Lennard-Jones and Coulomb interactions.<sup>34</sup> The NaK<sup>+</sup> bonding electron is treated fully quantum mechanically, with interactions described by pseudopotentials previously developed using the Phillips-Kleinman formalism.<sup>3</sup> The bonding electron's wavefunction is treated on a  $64 \times 64 \times 64$ grid. Gas-phase photodissociation trajectories were generated with a similar computational setup, except without the 254 THF solvent molecules. Simulations of single ions in the 254 THF solvents were simulated fully classically, and simulations of single quantum mechanical Na and K atoms in the 254 THF solvent molecules had their valence electron treated on a  $32 \times 32 \times 32$  grid to ensure the same grid density as in the NaK+ trajectories. The single ion/atom systems were allowed to propagate for at least 100 ps at ~298 K.<sup>23</sup> To generate equilibrium trajectories and thus calculate PMFs for the NaK+ system, we followed a similar method, using umbrella sampling to collect about 40-ps worth of dynamics at various fixed Na-K bond distances on the lowest excited electronic state.<sup>37</sup>

We generated initial configurations for 20 non-equilibrium MQC MD NaK<sup>+</sup>/THF excited-state trajectories by starting with ground-state equilibrium simulations run in the (N, V, T) ensemble at 298 K. We extracted uncorrelated (≥1-ps separation) configurations, while the ground-state NaK+ molecule was restrained to be coordinated by four THFs on the Na side and five THFs on the K side (chosen to ensure that our simulations did not mix coordination states with different molecular identities)<sup>11,23</sup> and then instantly placed the bonding electron onto the first excited electronic state while removing constraints on the solvent coordination number. These non-equilibrium excited-state trajectories were then allowed to propagate for at least 5 ps in the (N, V, E) ensemble. We only analyzed non-equilibrium data while the NaK+ bond distance was ≤8 Å to minimize finite-size effects, consistent with our previous work.<sup>23</sup> Additional simulation details are given in the supplementary material.

The key outcome of the NaK<sup>+</sup> photodissociation reaction that we wish to study is the reaction products: whether or not the bonding electron ends up associated with the Na<sup>+</sup> or K<sup>+</sup> photoproduct after the bond is broken. This makes the difference in charge between the Na and K photofragments a convenient order parameter for understanding the outcome of the reaction.

To proceed, we define the charge on each ion as the spherically integrated bonding electron density within a radial cut-off distance from its nucleus. To determine this distance, we used uncorrelated equilibrium configurations of isolated neutral Na and K atoms in liquid THF to obtain the pair distribution function, g(r), between the atoms and the THF center of masses (COMs) (as shown in the supplementary material). We performed similar calculations to obtain g(r)'s for isolated Na<sup>+</sup> and K<sup>+</sup> ions in liquid THF (also included in the supplementary material). Since the typical distribution of THF molecules around Na<sup>+</sup> and K<sup>+</sup> during the photodissociation process is in between that of the neutral atom and charged ion, we averaged the respective g(r)'s, obtaining the results shown in Fig. 2. We then chose the distance of the g(r) maxima as the cut-off distance over which to integrate the bonding electron charge, as indicated by the arrows at 3.5 Å for Na and 3.9 Å for K.

We also performed our analyses using two other sets of cutoff distances as well as a planar cut-off at the bond midpoint (as
described in the supplementary material) but found that the specific choice of cutoff did not qualitatively change any of our results
or conclusions. We note that by defining the charge associated with
each ion as that integrated over a finite-size sphere, the sum of the
charges on the two ions will not necessarily add to one (both because
of charge density outside the spheres as well as charge density that
appears in both spheres when they overlap, as also discussed in the
supplementary material). The cut-off distances we chose (3.5 Å for
Na and 3.9 Å for K) for the data presented here produce the smallest
amount of overlap compared to the other spherical cut-off distances

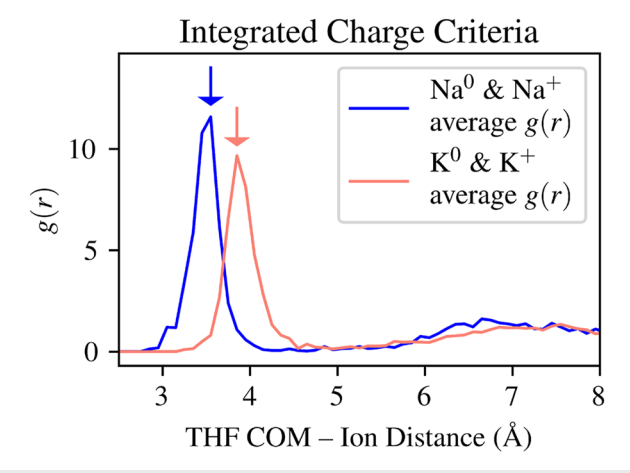


FIG. 2. Solvent-atom radial distribution functions (RDFs), averaged over both the neutral atoms and the bare ions, for THF center of mass (COM) around Na (blue curve) and K (pink curve). We used these RDFs to define the fractional charge associated with each ion as the integrated amount of charge density of the shared bonding electron inside the most probable distance between the THF COM and the ion, as indicated by the arrows (3.5 Å cut-off radius around Na and 3.9 Å cut-off radius around K)

explored in the supplementary material (Figs. S3 and S4). Using these cut-off distances, we monitor the charge difference between Na and K to examine how the different possible reaction products develop during bond dissociation.

#### **III. RESULTS AND DISCUSSION**

Figure 3 shows the fraction of the NaK<sup>+</sup> bonding electron's charge density on each atom (Na in blue, K in pink), defined as in Sec. II, as the bond distance between Na and K increases in the lowest electronic excited state. Since the ground-state NaK<sup>+</sup> equilibrium bond distance in the solution phase is different from that in the gas phase, <sup>11,23,32</sup> the Franck–Condon excitations start the gas-phase [panel (a)] and solution-phase [panel (c)] trajectories at different

# Charge Flow During NaK<sup>+</sup> Dissociation

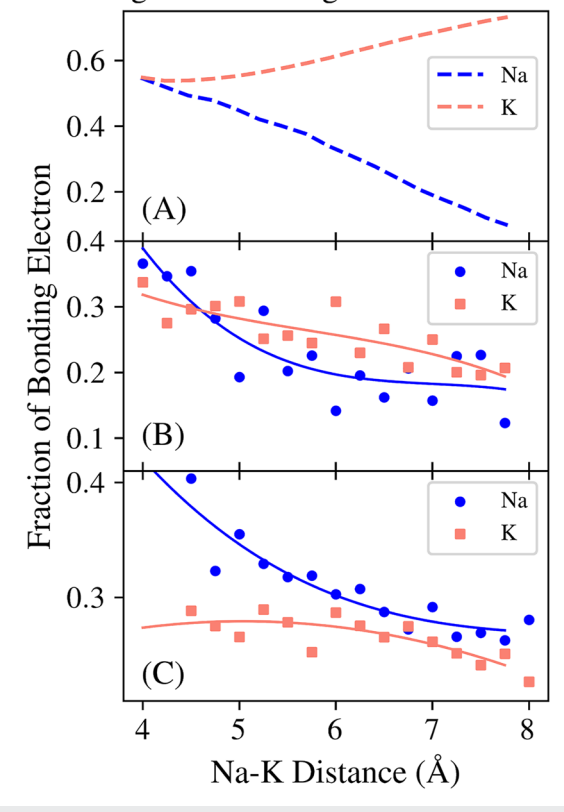


FIG. 3. Fraction of the bonding electron charge on Na (blue) and K (pink) on the lowest electronic excited state of NaK<sup>+</sup> in different environments. In the gas phase [dashed curves, panel (a)], the charge gradually localizes on K in the excited state as the bond lengthens because K has a lower electron affinity. In THF solution at equilibrium, the charge flow depends on the bond distance [panel (b)]: the charge first moves toward K as the bond reaches ~6 Å and then becomes more evenly shared as the bond distance approaches the PMF curve-crossing regime at ~9 Å separation.<sup>23</sup> During the non-equilibrium, dynamical dissociation process in gliquid THF, however, the charge prefers to reside on the Na fragment at all bond distances [panel (c)]. This is due to memory of the initial ground-state solvent configuration upon excitation, as there is insufficient time for solvent motions to come to equilibrium. The blue and pink curves in panels [(b) and (c)] are fitted trend lines to guide the eye, with parameters given in the supplementary material.

distances. The solution-phase equilibrium [panel (b)] charge separations are produced from excited-state umbrella sampling trajectories with the Na–K bond distance restrained, thus allowing us to access internuclear distances as low as 4 Å.

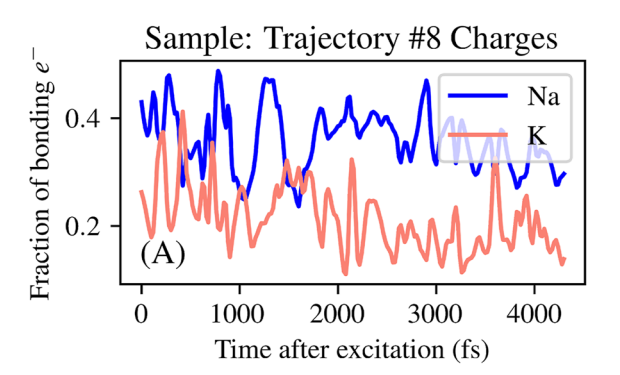
Upon photoexcitation in the gas phase [panel (a)], the bonding electron gradually localizes on the potassium fragment as the bond distance increases. If we perform the same NaK<sup>+</sup> excited-state dissociation in THF solution at equilibrium [panel (b)], we observe that at bond distances near the Franck–Condon region, equilibrium solvent fluctuations push electron density toward the K<sup>+</sup>, confirming the Na<sup>+</sup> + K<sup>0</sup> character predicted in our previous work.<sup>23</sup> As the bond separation approaches the PMF crossing regime near 9 Å (cf. Fig. 1), the bonding electron becomes split approximately evenly between the two fragment cations due to the strong mixing of the ground and excited-state free energy surfaces.<sup>23</sup>

However, when NaK<sup>+</sup> is photoexcited in liquid THF, the dissociation time scale is faster than the THF equilibration time. This means that the solvent molecules do not have time to reach their equilibrium configurations as the NaK<sup>+</sup> molecule separates so that memory of the initial ground-state solvent configuration is retained as the dissociation process proceeds. Figure 3(c) shows that the ground-state configuration in the Franck–Condon region has more electron charge density on the Na, a result of the greater electron affinity of Na. As a result, following photoexcitation, the shared electron remains primarily associated with the Na photofragment when the dissociation is performed dynamically in solution.

Comparing Figs. 3(b) and 3(c), we see that in the presence of liquid THF solvent molecules, the dynamics and even the products of the non-equilibrium photodissociation of NaK<sup>+</sup> are qualitatively different from what is expected if the solvent were able to maintain equilibrium throughout the bond-breaking process. This indicates that when studying solution-phase reactions, using the equilibrium PMF does not always accurately reflect the dynamical environment. Thus, unlike in the gas phase, where photodissociation reactions follow the dynamics predicted by PESs, one cannot necessarily use PMFs to predict dynamics in solution. This idea is supported by our previous work, which showed that potentials of mean force also do not capture other non-equilibrium phenomena, such as caging or the kinetic trapping of photofragments, due to local specific solvent interactions.<sup>10</sup>

Given that PMFs fail to describe even simple photodissociation reactions in solutions, we turn next to building a microscopic understanding of precisely how the non-equilibrium dynamics differ from those at equilibrium. We begin by examining the dynamical behavior of individual non-equilibrium photodissociation trajectories of NaK<sup>+</sup> in THF. We start by calculating the averages and standard deviations of the difference in the amount of charge on Na and K at each timestep,  $\langle q_{\rm Na}(t) - q_{\rm K}(t) \rangle$ , for each of the 20 dissociation trajectories. We then assign a trajectory as having the bonding electron associated with Na or K if the confidence interval of 80% of the standard deviation of  $\langle q_{\rm Na}(t) - q_{\rm K}(t) \rangle$  is entirely above or below 0, respectively. We classify trajectories where a 0 charge difference falls within this 80% confidence interval as fluctuating.

As an example of how our classification procedure works, Fig. 4(a) shows the fraction of the bonding electron associated with each ion for non-equilibrium photodissociation trajectory No. 8. We calculated  $q_{\rm Na}-q_{\rm K}$  at every time step and tabulated the mean and 80% of the standard deviation in Fig. 4(b) under trajectory No. 8;



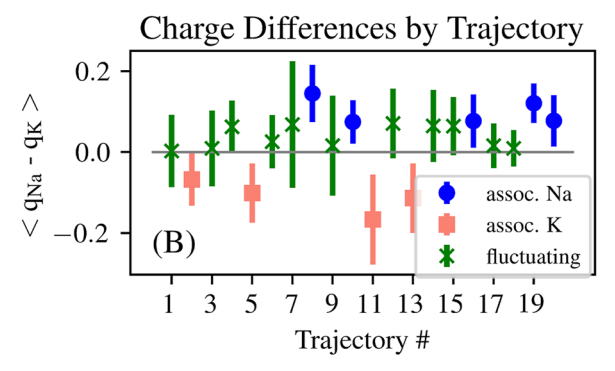


**FIG. 4.** Schematic of how the average difference in the amount of charge of the bonding electron on Na and on K is used to classify non-equilibrium photodissociation trajectories of NaK<sup>+</sup> in liquid THF. Panel (a) shows the difference in the instantaneous charge fractions on each atomic fragment for a particular trajectory (No. 8); for this example, the average charge difference favors Na by 0.145, with 80% of the standard deviation of 0.089. Panel (b) displays the averages (data points) and 80% of the standard deviation confidence intervals (error bars) for each of the 20 non-equilibrium trajectories. Trajectories in which the bonding electron mainly associates with Na are drawn with blue circles (5/20), those mainly associated with K are drawn with pink squares (4/20), and those that fluctuate between Na and K are drawn with green crosses (11/20).

since the average and confidence interval are entirely above 0, we then classify this trajectory as having the electron associated with Na. We also explored using different trajectory classification criteria, as discussed in the supplementary material, but found that although the precise numbers of trajectories in each class changed slightly, there was no qualitative difference in any of our subsequent analyses.

With this classification scheme, we find that the different trajectories in our non-equilibrium ensemble each show different directions of charge flow, with only a subset resembling the PMF prediction. Specifically, we observe three different non-equilibrium sub-ensembles: one where the bonding electron charge mainly associates with the Na fragment (5/20 trajectories, including trajectory No. 8), one where the charge mainly associates with the K fragment (4/20 trajectories), and one where the charge fluctuates roughly evenly between Na and K (the remaining 11/20 trajectories). The color scheme in Fig. 4(b) (blue circles for Na, pink squares for K, and green crosses for fluctuating) shows the classification of each trajectory into these three different non-equilibrium sub-ensembles. The

bonding electron in the fluctuating trajectories has a slight preference to associate with Na, on average, explaining the net association with Na for the entire non-equilibrium ensemble seen in Fig. 3(c).

We compare the fraction of bonding electron's charge on each ion as the Na<sup>+</sup>-K<sup>+</sup> bond distance increases for the three subensembles in Figs. 5(a), 5(c), and 5(e). When we take configurations from the trajectories that we label as "associated with Na," we see that the majority of the charge is near the Na fragment at all bond distances [Fig. 5(a)] and that the four "associated with K" trajectories have the bonding electron's charge mainly on K [Fig. 5(c)]. It is worth noting that the associated with Na and associated with K subensembles both behave differently than the gas-phase prediction, where the bonding electron localizes on K by 8 Å [Fig. 3(a)]. The associated with Na and K sub-ensembles also differ from the predictions at equilibrium in the solution phase, in which the electron is more evenly shared between Na and K [Fig. 3(b)].

For all of our non-equilibrium trajectories, we find that the electron's charge becomes more evenly shared as the bond length approaches 8 Å, near where the PMFs in Fig. 1 cross, suggesting that

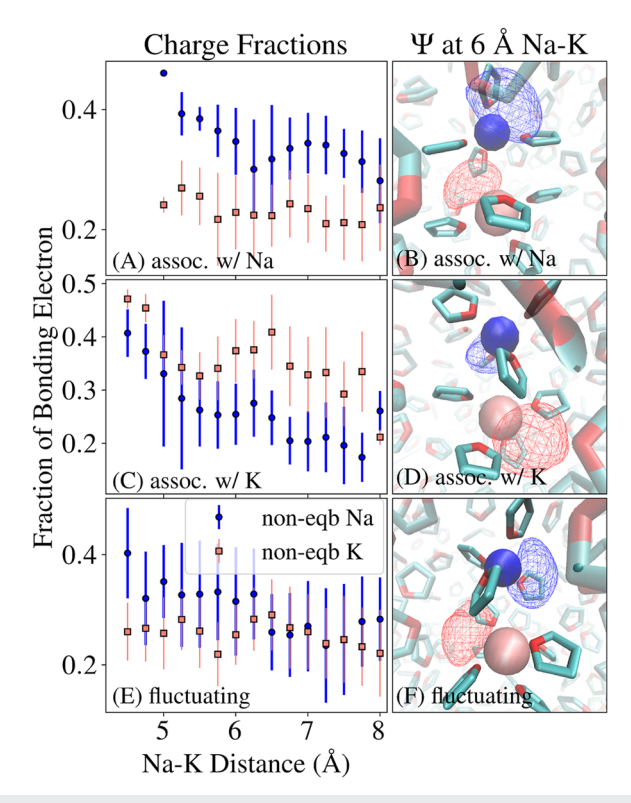
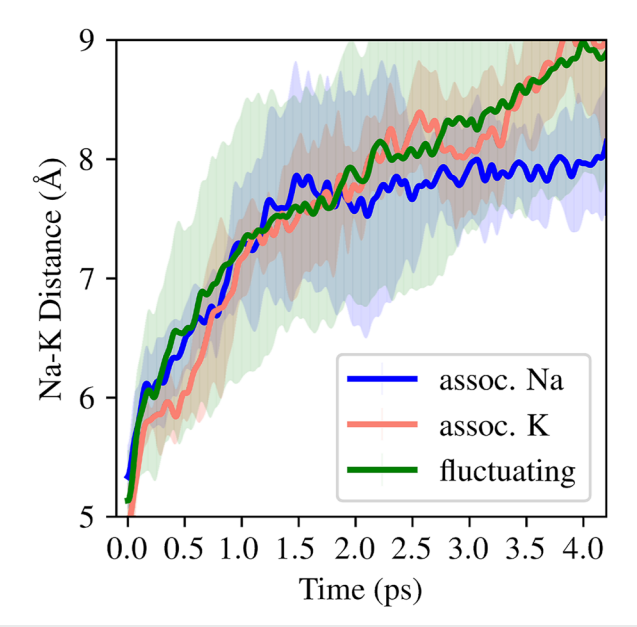


FIG. 5. Panels (a), (c), and (e) show the fraction of the bonding electron's charge on Na and on K as the Na–K bond distance increases during photodissociation for each of the three non-equilibrium sub-ensembles defined in Fig. 4(b). Panels (b), (d), and (f) show representative snapshots of the bonding electron's wavefunction for Na–K distances of 6 Å for each of the three non-equilibrium sub-ensembles. At shorter bond distances, before the solvent has had time to come to equilibrium, the sub-ensembles show qualitatively different trends compared to both the gas-phase and solution-phase equilibrium predictions in Fig. 3. Near the 8 Å bond distance limit, the charge separations begin to approach the equilibrium prediction, as the solvent has had more time to relax.

by the time the molecule is largely dissociated, the solvent is starting to approach equilibrium.

To get a better sense of the dissociation time scale, we show the average non-equilibrium Na–K bond distance (and the standard deviation as the error bars) at different times after promotion to the excited state for the three different sub-ensembles in Fig. 6. The rate of change in bond distance is similar for the associated with K and fluctuation sub-ensembles but decreases over time for the sub-ensemble of trajectories in which the charge is more associated with Na. Specifically, it takes about 2–2.5 ps for the associated with K and fluctuating sub-ensemble to reach 8 Å bond distance, while it takes roughly 3–3.5 ps for the Na sub-ensemble to reach this same distance. The longer time to approach the equilibrium prediction for the associated with Na sub-ensemble makes sense since this outcome is kinetically the farthest from the equilibrium prediction.

To better understand the local environment of the bonding electron in each of the three non-equilibrium sub-ensembles, Figs. 5(b), 5(d), and 5(f) display representative snapshots of the bonding electron wavefunction following photoexcitation of NaK<sup>+</sup> in liquid THF once the Na–K bond distance has reached 6 Å. For clarity, the first-shell THF molecules are colored solid, while the other THF molecules are transparent, and the wavefunction phases that are closer to Na are colored blue and those closer to K are colored pink (it is worth noting that the wavefunction phase colors do not precisely correspond to the integrated charge density). In panel B, the two lobes of the wavefunction are similar in size, but since one



**FIG. 6.** Average Na–K bond distance during the non-equilibrium photodissociation of NaK $^+$  as a function of time, color-coded by the different sub-ensembles defined in Fig. 4. In the associated with K (pink curve) and fluctuating (green curve) sub-ensembles, the rate of the Na–K bond distance increase is roughly constant up to  $\sim$ 4 ps. However, in the associated with Na sub-ensemble (blue curve), the rate of change in bond distance decreases with time, particularly after  $\sim$ 2 ps. The shaded regions show the standard deviation of the distances averaged over the trajectories in each sub-ensemble.

lobe is on the far side of the Na atom from the K atom while the other lobe lies between the two atoms (albeit closer to K), the integrated charge lies more heavily on Na. In panel D, the wavefunction lobe closer to K is significantly larger than that closer to Na, resulting in a greater fraction of the bonding electron on K. In the fluctuating trajectories, panel F, the two lobes are similar in size and about equally distributed between the two ions.

We have argued in previous work that the way an electron distributes itself near a cation in liquid THF depends on the number of THF molecules involved in making dative bonds to the cation. <sup>23,38–40</sup> This suggests that the different behaviors seen in the different non-equilibrium sub-ensembles might result from changes in the coordination of THFs to the cationic fragments formed as the NaK<sup>+</sup> molecule dissociates.

Thus, we examine the effects of solvent coordination on the bonding electron charge flow in Fig. 7; we define a THF molecule as being in a dative bond with one of the cation cores using a distance-based criterion, as in previous work.  $^{11,12,23,32}$  The average Na $^+$  and K $^+$  coordination numbers for the solution-phase excited-state equilibrium system are presented with dashed curves (same in all three panels for reference). The data show that when the solvent molecules have sufficient time to equilibrate, the number of THFs coordinated to Na $^+$  increases from around 4 in the Franck–Condon region to  $\sim\!5.5$  when the bond is stretched to  $\sim\!8$  Å, while the number of THFs coordinated to K $^+$  increases from  $\sim\!5$  to near 6 over this same range of bond lengths. We note that the typical time scale for fluctuations in the dative bond coordination number is of order 1 ps, as discussed in more detail in the supplementary material.

In the associated with Na sub-ensemble [Fig. 7(a)], neither the  $K^+$  nor the Na $^+$  coordination numbers follow the equilibrium predictions, with the coordination of Na $^+$  deviating more significantly. This suggests that in this sub-ensemble, the solvent fluctuations around both ions take place on time scales longer than the bond dissociation, and these trajectories retain memory of their initial configuration upon excitation; in other words, the solvents remain oriented to favor having the bonding electron associated with Na.

In contrast, in the associated with K sub-ensemble [Fig. 7(b)], the sodium coordination number eventually increases enough to reach its equilibrium prediction at distances longer than ~7 Å, while the potassium coordination number follows similar dynamics as in the Na sub-ensemble. As a result, the additional THF near Na pushes the bonding electron density closer to K [cf. Fig. 5(d)], leading to more integrated charge on K. In addition, the equilibrium prediction is that when the bond distance is ~5 Å, an additional THF is coordinated to the Na<sup>+</sup> [panel (b) blue dashed curve], which keeps the charge more evenly split between the two ions. However, during the dynamical process, this additional THF does not coordinate to the Na<sup>+</sup> until the bond distance reaches 7 Å [panel (b), blue error bars], which takes about 1 ps after photodissociation (cf. Fig. 6). This delay leads to a different behavior compared to equilibrium predictions.

Finally, in the fluctuating sub-ensemble [Fig. 7(c)], the sodium coordination number remains around 4–4.5 THFs, while the potassium coordination number closely follows the equilibrium prediction. Although there is a slight increase in average THF coordination number around sodium near 7 Å bond distance, the increase is not as significant as it is in the K sub-ensemble around the same distance. In addition, the Na<sup>+</sup> coordination number later drifts down again without ever reaching the equilibrium prediction. The



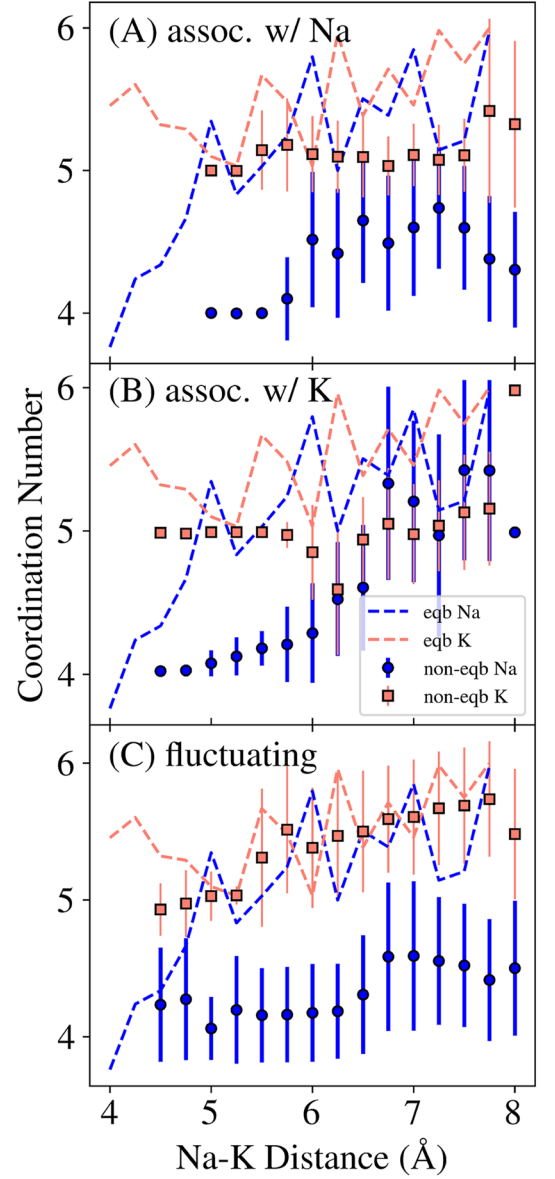


FIG. 7. Number of THF molecules datively coordinated to Na (blue) and K (pink) during non-equilibrium NaK<sup>+</sup> dissociation (data points with error bars) and at equilibrium on the electronic excited state (dashed curves, same in all three panels) as a function of Na–K bond distance; the three panels show the data for the three non-equilibrium sub-ensembles defined in Fig. 4(b). The associated with Na subensemble has neither ion's coordination number match the equilibrium prediction [panel (a)], while in the associated with K sub-ensemble [panel (b)], the Na coordination number reaches its equilibrium value, pushing more electron density onto K. Finally, the fluctuating trajectories [panel (c)] have a K coordination number that closely matches equilibrium but a Na coordination number that is much lower.

solvent coordination around potassium, however, is similar to the equilibrium prediction from the beginning of the dissociation process. Figure S10 in the supplementary material displays the persistence of THF coordination (coordination number autocorrelation

function) around each ion at the Franck–Condon bond distance region. Even though the Na $^+$  and K $^+$  coordination number fluctuations are both of order 1 ps, the sodium coordination number still plays a more important role as to whether the final dissociation product is able to follow the equilibrium prediction, likely because the Na $^+$ -THF dative bond is about five times stronger than the K $^+$ -THF dative bond.

None of the sub-ensembles displays a dynamical coordination number resembling the equilibrium prediction for both ions, further emphasizing that the dissociation time scale is shorter than the solvent relaxation time. Thus, relying on the equilibrium PMFs cannot accurately describe the dynamics of solution-phase bond-breaking reactions, such as this one. We note that in addition to the number of first-shell solvents, the orientations of these first-shell THF molecules also play a minor role in creating a more favorable environment for the electron to be associated with either ion, and this analysis is included in the supplementary material.

There are two possible general factors that could be responsible for the fact that the equilibrium PMFs do not adequately describe the dynamical bond dissociation. First, of necessity, the PMF assumes that the solvent has had infinite time to equilibrate with the solute at each bond distance, but the solvent fluctuations may be memory-dependent (in the sense of needing to be described by the generalized Langevin equation). This means that the non-equilibrium velocity of the dissociating fragments could cause them to experience a different local effective solvent friction than if the fragments were not moving. Second, the presence of the solvent causes mixing of the solute's (gas-phase) electronic surfaces, as is evident from the fact that the gas-phase surfaces do not cross while the PMFs do cross near 9 Å. The extent of this solvent-induced mixing could be different between the non-equilibrium system and that at equilibrium so that the effective potential energy surface is different.

As a preliminary exploration of how each of these potential reasons contributes to the failure of the PMF to describe solutionphase bond-breaking dynamics, we investigate the equilibrium and non-equilibrium solvent-induced coupling between the ground- and excited-state energy surfaces (see Fig. S12 and the corresponding discussion in the supplementary material). We accomplish this by constructing an effective non-equilibrium energy surface based on Jarzynski's time integral of work formalism, 42 similar to what we have used in previous work, 10 and then back-calculating the coupling between the different solution-phase energy surfaces and those in the gas phase. We find that the difference between the bond-distance-dependent coupling matrix elements during nonequilibrium dissociation and at equilibrium is relatively small. This strongly suggests that dynamical solvent memory effects are important in explaining why the equilibrium PMF is unable to correctly predict the non-equilibrium dynamics.

## IV. CONCLUSIONS

In summary, we have shown that for bond-breaking reactions in solution, non-equilibrium dynamics can be qualitatively different from equilibrium, since the reactants can retain memory of their initial solvent configuration for a longer period of time than it takes to dissociate. We showed that upon photoexcitation of ground-state  $NaK^+$  in liquid THF, the solvent does not have enough time to relax to its equilibrium geometry. As a result, the excited  $NaK^+$ 

molecule retains memory of its ground-state configuration, causing the bonding electron to remain more associated with Na, which is the opposite outcome of what would be predicted by the equilibrium PMFs. We argued that solute velocity-dependent solvent memory effects are an important factor in explaining the difference between equilibrium and non-equilibrium dissociation dynamics.

In our detailed exploration of the dissociation dynamics, we found that the non-equilibrium trajectories could be separated into three distinct sub-categories, with about a quarter of the trajectories having the bonding electron more associated with Na during the dissociation process, another quarter with the charge more associated with K, and about half with the charge generally evenly shared. These sub-categories arise mainly due to differences in the first-shell THF coordination number of the two ions during dissociation.

The net conclusion is that even though the solvent molecules have relatively weak interactions with the photofragments, the solvent is still unable to fully equilibrate during the dissociation process. We note that in previous work studying a similar bond-breaking reaction in liquid Ar, we found that for the PMF predictions to provide a useful predictor of non-equilibrium dynamics, it was necessary to shorten the time scale of solvent fluctuations by decreasing the solvent mass by a factor of 20. <sup>10</sup> The current study emphasizes that even for molecular solvents that have local specific interactions with solutes, solution-phase reactions still deviate from their equilibrium predictions, reflecting the inherently complex nature of chemical reactivity in liquids.

It makes sense, based on previous simulation work, that linear response predictions where non-equilibrium solvation dynamics follow the equilibrium prediction are more inaccurate with smaller solutes that are better able to "feel" the molecularity of the solvent. 43 Simulation studies of PMF calculations for S<sub>N</sub>1 fragmentation also concluded that the solvation structure greatly influences reaction progress. 44 Since we found that even solvents that have weak interactions with solutes cannot fully equilibrate during bond dissociation, we expect this effect to be more significant for reactions such as S<sub>N</sub>1, where the solvent plays a direct role in stabilizing the intermediate. Overall, PMF predictions rely on the assumption that the solvent relaxation is fast enough that they remain equilibrated as the reaction progresses. However, this is not the case for the photodissociation of diatomics with relatively weak solute-solvent specific interactions. This suggests that PMFs would be even less accurate with reactions involving multiple sites, conformational changes, or stronger solute-solvent interactions, which are all common in solution-phase chemistry.

## SUPPLEMENTARY MATERIAL

The supplementary material includes the g(r)'s for THF around a single Na atom, a single K atom, a single Na ion, and a single K atom, which were used in the averages presented in Fig. 2; the fraction of the bonding electron on each ion for the 20 individual non-eqb trajectories; fitting parameters for the trend curves in Figs. 3(b) and 3(c); an analysis of how things change using alternative radius cutoffs for charge measurements; an analysis using alternative charge measurements that ensure a unity sum of the fractional charge on each ion; an analysis using alternative classifications of the three non-equilibrium ensembles; a discussion of how the average bond distance changes with time for each

non-equilibrium sub-ensemble; an analysis of the first-shell solvent molecule orientations, and an analysis of the solvent coordination number fluctuations. All of the trajectory data are available in a Dryad repository (DOI: 10.5061/dryad.vhhmgqp63), including the raw xyz trajectory files, the excited-state wavefunction cube files, and the first-shell THF coordination numbers.

#### **ACKNOWLEDGMENTS**

This work was supported by the U.S. Department of Energy, Basic Energy Sciences, Condensed-Phase and Interfacial Molecular Sciences Program, under Grant No. DE-SC0017800. Computational resources were provided by the UCLA Institute for Digital Research and Education.

#### **AUTHOR DECLARATIONS**

#### **Conflict of Interest**

The authors have no conflicts to disclose.

#### **Author Contributions**

Hannah Y. Liu: Data curation (lead); Formal analysis (supporting); Investigation (supporting); Methodology (equal); Software (equal); Writing – original draft (lead); Writing – review & editing (supporting). Kenneth J. Mei: Investigation (supporting); Methodology (equal); Software (equal). William R. Borrelli: Investigation (supporting); Methodology (supporting); Writing – review & editing (supporting). Benjamin J. Schwartz: Conceptualization (lead); Funding acquisition (lead); Project administration (lead); Supervision (lead); Writing – review & editing (lead).

# **DATA AVAILABILITY**

In addition to the material available in the supplementary material, all of the simulation data are available in a Dryad repository (DOI: 10.5061/dryad.vhhmgqp63), including the raw xyz trajectory files, the excited-state wavefunction cube files, and the first-shell THF coordination numbers.

# **REFERENCES**

- <sup>1</sup> M. Born and W. Heisenberg, "Zur quantentheorie der molekeln," in *Original Scientific Papers Wissenschaftliche Originalarbeiten*, Werner Heisenberg Gesammelte Werke Collected Works Vol. A / 1, edited by W. Blum, H. Rechenberg, and H. P. Dürr (Springer, Berlin, Heidelberg, 1985), pp. 216–246.
- <sup>2</sup>W. Heitler and F. London, "Wechselwirkung neutraler atome und homöopolare bindung nach der quantenmechanik," Z. Phys. 44, 455–472 (1927).
- <sup>3</sup>H. Mustroph, "Potential-energy surfaces, the Born-Oppenheimer approximations, and the Franck-Condon principle: Back to the roots," ChemPhysChem 17, 2616–2629 (2016).
- <sup>4</sup>H. B. Schlegel, "Exploring potential energy surfaces for chemical reactions: An overview of some practical methods," J. Comput. Chem. **24**, 1514–1527 (2003).
- <sup>5</sup>C. J. Bardeen, J. Che, K. R. Wilson, V. V. Yakovlev, V. A. Apkarian, C. C. Martens, R. Zadoyan, B. Kohler, and M. Messina, "Quantum control of I<sub>2</sub> in the gas phase and in condensed phase solid Kr matrix," J. Chem. Phys. **106**, 8486–8503 (1997)
- <sup>6</sup>J. Franck and E. Rabinowitsch, "Some remarks about free radicals and the photochemistry of solutions," Trans. Faraday Soc. **30**, 120–130 (1934).

- <sup>7</sup>R. Zadoyan, Z. Li, C. C. Martens, and V. A. Apkarian, "The breaking and remaking of a bond: Caging of I<sub>2</sub> in solid Kr," J. Chem. Phys. **101**, 6648–6657 (1994).
- <sup>8</sup>V. S. Batista and D. F. Coker, "Nonadiabatic molecular dynamics simulation of photodissociation and geminate recombination of I<sub>2</sub> liquid xenon," J. Chem. Phys. **105**, 4033–4054 (1996).
- <sup>9</sup>P. Slavíček, P. Žďánská, P. Jungwirth, R. Baumfalk, and U. Buck, "Size effects on photodissociation and caging of hydrogen bromide inside or on the surface of large inert clusters: From one to three icosahedral argon layers," J. Phys. Chem. A 104, 7793–7802 (2000).
- <sup>10</sup> A. Vong, D. R. Widmer, and B. J. Schwartz, "Nonequilibrium solvent effects during photodissociation in liquids: Dynamical energy surfaces, caging, and chemical identity," J. Phys. Chem. Lett. 11, 9230–9238 (2020).
- <sup>11</sup>D. R. Widmer and B. J. Schwartz, "Solvents can control solute molecular identity," Nat. Chem. **10**, 910–916 (2018).
- <sup>12</sup>D. R. Widmer and B. J. Schwartz, "The role of the solvent in the condensed-phase dynamics and identity of chemical bonds: The case of the sodium dimer cation in THF," J. Phys. Chem. B 124, 6603–6616 (2020).
- <sup>13</sup>W. J. Glover, R. E. Larsen, and B. J. Schwartz, "How does a solvent affect chemical bonds? Mixed quantum/classical simulations with a full ci treatment of the bonding electrons," J. Phys. Chem. Lett. 1, 165–169 (2010).
- <sup>14</sup>A. C. Moskun and S. E. Bradforth, "Photodissociation of ICN in polar solvents: Evidence for long lived rotational excitation in room temperature liquids," J. Chem. Phys. 119, 4500–4515 (2003).
- <sup>15</sup>H. Jin, M. Liang, S. Arzhantsev, X. Li, and M. Maroncelli, "Photophysical characterization of benzylidene malononitriles as probes of solvent friction," J. Phys. Chem. B **114**, 7565–7578 (2010).
- <sup>16</sup>G. H. Peslherbe, R. Bianco, J. T. Hynes, and B. M. Ladanyi, "On the photodissociation of alkali-metal halides in solution," J. Chem. Soc., Faraday Trans. 93, 977–988 (1997).
- $^{17}$ D. M. Koch and G. H. Peslherbe, "Importance of polarization in quantum mechanics/molecular mechanics descriptions of electronic excited states: NaI ( $\rm H_2O$ ) $_n$  photodissociation dynamics as a case study," J. Phys. Chem. B 112, 636–649 (2008).
- <sup>18</sup>I. Burghardt, L. S. Cederbaum, and J. T. Hynes, "Environmental effects on a conical intersection: A model study," Faraday Discuss. 127, 395–411 (2004).
- <sup>19</sup> N. Yu, C. J. Margulis, and D. F. Coker, "Influence of solvation environment on excited state avoided crossings and photodissociation dynamics," J. Phys. Chem. B 105, 6728–6737 (2001).
- $^{20}$ B. Ensing, E. J. Meijer, P. Blöchl, and E. J. Baerends, "Solvation effects on the  $S_N2$  reaction between  $CH_3Cl$  and  $Cl^-$  in water," J. Phys. Chem. A **105**, 3300–3310 (2001).
- <sup>21</sup>C. K. Regan, S. L. Craig, and J. I. Brauman, "Steric effects and solvent effects in ionic reactions," Science **295**, 2245–2247 (2002).
- $^{22}$  Y. Li and B. Hartke, "Assessing solvation effects on chemical reactions with globally optimized solvent clusters," <code>ChemPhysChem 14</code>, 2678–2686 (2013).
- Ž<sup>3</sup>K. J. Mei and B. J. Schwartz, "How solvation alters the thermodynamics of asymmetric bond-breaking: Quantum simulation of NaK<sup>+</sup> in liquid tetrahydrofuran," J. Phys. Chem. Lett. **15**, 8187–8195 (2024).
- <sup>24</sup>A. Valance, "Adiabatic potential energies for NaK<sup>+</sup>, NaRb<sup>+</sup>, NaCs<sup>+</sup>, KRb<sup>+</sup>, KCs<sup>+</sup>, RbCs<sup>+</sup>, Na<sub>2</sub><sup>+</sup>, K<sub>2</sub><sup>+</sup>, Rb<sub>2</sub><sup>+</sup>, and Cs<sub>2</sub><sup>+</sup> molecular ions," J. Chem. Phys. **69**, 355–366 (1978).
- <sup>25</sup> A. Valance, A. Bernier, and M. El Maddarsi, " $\sigma$  and  $\pi$  molecular states for NaK<sup>+</sup>, KRb<sup>+</sup> and NaRb<sup>+</sup> molecular ions," Chem. Phys. **103**, 151–162 (1986).
- <sup>26</sup>M. Musiał, A. Bewicz, P. Skupin, and S. A. Kucharski, "Potential energy curves for the LiK<sup>+</sup> and NaK<sup>+</sup> molecular ions with the coupled cluster method," in *Advances in Quantum Chemistry* (Elsevier, 2018), Vol. 76, pp. 333–349.
- <sup>27</sup>M. Ciocca, C. E. Burkhardt, J. J. Leventhal, and T. Bergeman, "Precision Stark spectroscopy of sodium: Improved values for the ionization limit and bound states," Phys. Rev. A 45, 4720–4730 (1992).
- <sup>28</sup>C.-J. Lorenzen, K. Niemax, and L. R. Pendrill, "Precise measurements of 39 K nS and nD energy levels with an evaluated wavemeter," Opt. Commun. 39, 370–374 (1981).
- <sup>29</sup>H. B. Gray and J. R. Winkler, "Long-range electron transfer," Proc. Natl. Acad. Sci. U. S. A. 102, 3534–3539 (2005).

- <sup>30</sup> J. R. Winkler and H. B. Gray, "Long-range electron tunneling," J. Am. Chem. Soc. 136, 2930–2939 (2014).
- <sup>31</sup> J. G. Kirkwood, "Statistical mechanics of fluid mixtures," J. Chem. Phys. 3, 300–313 (1935).
- <sup>32</sup> A. Vong, K. J. Mei, D. R. Widmer, and B. J. Schwartz, "Solvent control of chemical identity can change photodissociation into photoisomerization," J. Phys. Chem. Lett. 13, 7931–7938 (2022).
- <sup>33</sup> J. Chandrasekhar and W. L. Jorgensen, "The nature of dilute solutions of sodium ion in water, methanol, and tetrahydrofuran," J. Chem. Phys. 77, 5080–5089 (1982).
- (1982).

  34 M. P. Allen and D. J. Tildesley, *Computer Simulation of Liquids* (Oxford University Press, 2017).
- <sup>35</sup>C. J. Smallwood, R. E. Larsen, W. J. Glover, and B. J. Schwartz, "A computationally efficient exact pseudopotential method. I. Analytic reformulation of the Phillips–Kleinman theory," J. Chem. Phys. 125, 074102 (2006).
- <sup>36</sup>C. J. Smallwood, C. N. Mejia, W. J. Glover, R. E. Larsen, and B. J. Schwartz, "A computationally efficient exact pseudopotential method. II. application to the molecular pseudopotential of an excess electron interacting with tetrahydrofuran (THF)," J. Chem. Phys. 125, 074103 (2006).

- <sup>37</sup>G. M. Torrie and J. P. Valleau, "Nonphysical sampling distributions in Monte Carlo free-energy estimation: Umbrella sampling," J. Comput. Phys. 23, 187–199 (1977).
- <sup>38</sup>W. J. Glover, R. E. Larsen, and B. J. Schwartz, "Nature of sodium atoms/(Na<sup>+</sup>, e<sup>-</sup>) contact pairs in liquid tetrahydrofuran," J. Phys. Chem. B 114, 11535–11543 (2010).
- <sup>39</sup>W. J. Glover, R. E. Larsen, and B. J. Schwartz, "Simulating the formation of sodium:electron tight-contact pairs: Watching the solvation of atoms in liquids one molecule at a time," J. Phys. Chem. A 115, 5887–5894 (2011).
- <sup>40</sup> A. E. Bragg, W. J. Glover, and B. J. Schwartz, "Watching the solvation of atoms in liquids one solvent molecule at a time," Phys. Rev. Lett. **104**, 233005 (2010).
- <sup>41</sup>E. Cortés, B. J. West, and K. Lindenberg, "On the generalized Langevin equation: Classical and quantum mechanical," J. Chem. Phys. **82**, 2708–2717 (1985).
- <sup>42</sup>C. Jarzynski, "Nonequilibrium equality for free energy differences," Phys. Rev. Lett. 78, 2690–2693 (1997).
- <sup>43</sup>T. Fonseca and B. M. Ladanyi, "Breakdown of linear response for solvation dynamics in methanol," J. Phys. Chem. **95**, 2116–2119 (1991).
- $^{44}$ D. S. Hartsough and K. M. J. Merz, "Potential of mean force calculations on the  $S_{\rm N}1$  fragmentation of *tert*-butyl chloride," J. Phys. Chem. **99**, 384–390 (1995).